COMMUNICATIONS IN COMPUTATIONAL PHYSICS
Vol. **1**, No. 3, pp. 479-493

Commun. Comput. Phys.
June 2006

Numerical Method for the Deterministic Kardar-Parisi-Zhang Equation in Unbounded Domains

Zhenli Xu[1,*], Houde Han[2] and Xiaonan Wu[3]

[1] *Department of Mathematics, University of Science and Technology of China, Hefei 230026, P.R. China.*
[2] *Department of Mathematical Sciences, Tsinghua University, Beijing 100084, P.R. China.*
[3] *Department of Mathematics, Hong Kong Baptist University, Kowloon Tong, Hong Kong.*

Received 25 July 2005; Accepted (in revised version) 24 September 2005

Abstract. We propose an artificial boundary method for solving the deterministic Kardar-Parisi-Zhang equation in one-, two- and three dimensional unbounded domains. The exact artificial boundary conditions are obtained on the artificial boundaries. Then the original problems are reduced to equivalent problems in bounded domains. A finite difference method is applied to solve the reduced problems, and some numerical examples are provided to show the effectiveness of the method.

Key words: Quasilinear parabolic equation; artificial boundary condition; viscous Hamilton-Jacobi equation; unbounded domain.

1 Introduction

Surface growth is a class of important problems arising from many practical applications [22], such as molecular beam epitaxy, bacterial growth, fluid flow in porous media or evolution of fire fronts, etc. During the recent two decades, many models based on stochastic partial differential equations have been developed to simulate the mechanism of surface growth. Among these, one of the most well known models is the one introduced by Kardar, Parisi and Zhang (KPZ) [18],

$$u_t = \nu\Delta u + \lambda|\nabla u|^2 + \eta, \tag{1.1}$$

where $u = u(x,t)$ represents the height of surface growth at $d-$dimensional position x

*Correspondence to: Zhenli Xu, Department of Mathematics, University of Science and Technology of China, Hefei 230026, P.R. China. Email: xuzl@ustc.edu

and time t, ν and λ are the parameters of diffusion and nonlinear terms, respectively. The last term of the equation (1.1), $\eta = \eta(x,t)$, is a Gaussian white noise which is produced by a stochastic force.

The KPZ equation is the first continuum partial differential equation to model the dynamics of surface growth. Based on it numerous studies have been carried out by many authors. Among them a relevant problem is to study the dynamics of the KPZ equation without noise term, which describes the relaxation of an initially rough surface to a flat one.

In this paper, we study the initial boundary value problem of the deterministic KPZ equations with a source term in unbounded domains,

$$u_t = \Delta u + |\nabla u|^2 + f(x,t), \quad \text{in } \mathbb{R}^d \times (0,T] \tag{1.2}$$

$$u(x,0) = u_0(x), \quad x \in \mathbb{R}^d, \tag{1.3}$$

$$u \to 0, \quad \text{when } |x| \to +\infty, \tag{1.4}$$

where $d = 1, 2$, or 3, and the initial value $u_0(x)$ and the source term $f(x,t)$ vanish outside a d-dimensional ball $B_0^d = \{x : |x| \le R\}$, namely,

$$\text{supp}\{f(x,t)\} \subset B_0^d \times [0,T], \quad \text{supp}\{u_0(x)\} \subset B_0^d. \tag{1.5}$$

For the numerical solution of problem (1.2)-(1.4), we need to introduce artificial boundaries to make the domain finite, to find the artificial boundary conditions, and to reduce the original problem to an equivalent problem on a bounded domain. The so-called artificial boundary method has been the most efficient method for the numerical solution of PDEs in an unbounded domain, including applications to wave equations [3, 8, 9, 19], elliptic equations [4,11,12,25] and, most relevant to the current work, the parabolic equations [7, 13,14,21,24], etc. In general, the basic assumption of the artificial boundary method is that the equation is linear. Consequently, certain analytic forms of the boundary conditions on the artificial boundaries can be obtained. Usually, the artificial boundary method cannot be applied directly to nonlinear problems. However, for some problems, if the equation can be linearized outside the artificial boundaries, then it is possible to find the boundary conditions on the artificial boundaries [5,10,15].

The artificial boundary method of the KPZ equation is an extension of the existing method for linear parabolic equations. Because the source term $f(x,t)$ is compact, the KPZ equation (1.2) can be transformed into a linear parabolic equation in the exterior domain where the artificial boundary condition can be derived. After transforming it back into the original variable, we can solve the problem on the finite domain. In the one-dimensional case, we have used this idea to solve the Burgers equation in unbounded domains [16].

Many numerical methods have been used for solving the stochastic KPZ equation (1.1) in bounded domains, such as finite difference methods and their improved versions [1,20], pseudospectral methods [6] etc. For the deterministic equation, an effective method is the second order Crank-Nicolson scheme. The stability and convergence for the artificial

boundary method for the parabolic equation are proposed in Wu and Sun [24]. It is also unconditionally stable for the KPZ equation which is demonstrated in our numerical examples. The deterministic KPZ equation (1.2) is often referred to as a simplest model equation of the viscous Hamilton-Jacobi equation which has attracted much interest in recent years (see [2, 26]).

The organization of this paper is as follows. In Section 2, we present exact and approximating artificial boundary conditions of the KPZ equation in one-, two- and three-dimensional spaces. In Section 3, finite difference discretizations are discussed. Some numerical results will be presented in the final section.

2 Artificial boundary conditions

Denote by $\Gamma = \partial B_0^d$ the artificial boundary and $\Omega_e = \mathbb{R}^d \setminus B_0^d$ by the exterior domain. In order to obtain boundary conditions on the artificial boundary Γ, we consider firstly the restriction of u on the exterior domain Ω_e. It follows from the condition (1.5) that the problem (1.2)-(1.4) satisfies

$$u_t = \Delta u + |\nabla u|^2, \quad \text{in } \Omega_e \times (0, T] \tag{2.1}$$

$$u(x, 0) = 0, \quad x \in \Omega_e, \tag{2.2}$$

$$u \to 0, \quad \text{when } |x| \to +\infty. \tag{2.3}$$

If we assume that the boundary condition $u(x,t)|_\Gamma$ is given, the above is a well-posed problem. By the Cole-Hopf transformation $v = e^u - 1$, the problem (2.1)-(2.3) can be transformed into a linear problem [23],

$$v_t = \Delta v, \quad \text{in } \Omega_e \times (0, T] \tag{2.4}$$

$$v(x, 0) = 0, \quad x \in \Omega_e, \tag{2.5}$$

$$v \to 0, \quad \text{when } |x| \to +\infty, \tag{2.6}$$

which can be solved together with the corresponding boundary condition on Γ.

In the one-dimensional case $d = 1$, the exterior domain Ω_e consists of two semi-infinite parts $\Omega_l = \{x : x < -R\}$ and $\Omega_r = \{x : x > R\}$. Consider the problem (2.4)-(2.6) on the right part Ω_r. It can be verified that the solution $v(x,t)$ is

$$v(x,t) = \frac{x-R}{2\sqrt{\pi}} \int_0^t v(R,\tau) \frac{e^{-(x-R)^2/4(t-\tau)}}{(t-\tau)^{3/2}} d\tau. \tag{2.7}$$

From the formula (2.7), a relationship between $\frac{\partial v}{\partial x}$ and $\frac{\partial v}{\partial t}$ was obtained by Han and Huang [13], namely,

$$\frac{\partial v(R,t)}{\partial x} = -\frac{1}{\sqrt{\pi}} \int_0^t \frac{\partial v(R,\tau)}{\partial \tau} \frac{1}{\sqrt{t-\tau}} d\tau. \tag{2.8}$$

A similar relationship can also be obtained on the left boundary $x=-R$,

$$\frac{\partial v(-R,t)}{\partial x}=\frac{1}{\sqrt{\pi}}\int_0^t\frac{\partial v(-R,\tau)}{\partial\tau}\frac{1}{\sqrt{t-\tau}}d\tau. \tag{2.9}$$

When transforming them back into the original variable, we obtain the nonlinear artificial boundary conditions of the one dimensional KPZ equation

$$\frac{\partial u(R,t)}{\partial x}=-\frac{1}{\sqrt{\pi}}\int_0^t\frac{\partial u(R,\tau)}{\partial\tau}\frac{e^{u(R,\tau)-u(R,t)}}{\sqrt{t-\tau}}d\tau, \tag{2.10}$$

$$\frac{\partial u(-R,t)}{\partial x}=\frac{1}{\sqrt{\pi}}\int_0^t\frac{\partial u(-R,\tau)}{\partial\tau}\frac{e^{u(-R,\tau)-u(-R,t)}}{\sqrt{t-\tau}}d\tau. \tag{2.11}$$

2.1 The two-dimensional KPZ equation

We now concentrate on the two-dimensional case $d=2$. Let D be a bounded domain in B_0^2 and $\Omega_i=B_0^2\setminus\bar{D}$ the computational domain. We consider the following initial boundary value problem in the bounded domain Ω_i with the polar coordinates:

$$u_t=u_{rr}+u_r^2+\frac{1}{r}u_r+\frac{1}{r^2}(u_{\theta\theta}+u_\theta^2)+f(r,\theta,t), \quad \text{in } \Omega_i\times(0,T], \tag{2.12}$$

$$u|_{\partial D}=g(r,\theta,t), \quad \text{in } \partial\Omega\times(0,T], \tag{2.13}$$

$$u(r,\theta,0)=u_0(r,\theta,0), \quad \text{in } \Omega_i, \tag{2.14}$$

$$u|_\Gamma=u(R,\theta,t), \tag{2.15}$$

where the artificial boundary condition $\Gamma=\{(r,\theta):r=R,0\le\theta<2\pi\}$ is a circle and $u(R,\theta,t)$ is unknown. In order to obtain the artificial condition on Γ, consider the restriction of the solution on the unbounded domain Ω_e, in which the KPZ equation can be transformed into a parabolic equation [23] by the Cole-Hopf transformation $v=e^u-1$,

$$v_t=v_{rr}+\frac{1}{r}v_r+\frac{1}{r^2}v_{\theta\theta} \tag{2.16}$$

$$v(r,\theta,0)=0, \tag{2.17}$$

$$v\to 0, \quad \text{when } r\to+\infty, \tag{2.18}$$

$$v|_\Gamma=v(R,\theta,t). \tag{2.19}$$

To solve this problem, we look for the solution of the form

$$v(r,\theta,t)=v_0(r,t)+\sum_{m=1}^{\infty}\alpha_m(r,t)\cos m\theta+\beta_m(r,t)\sin m\theta. \tag{2.20}$$

Substituting the above form into (2.16), we obtain

$$\begin{aligned}\frac{\partial v_0}{\partial t}-\frac{\partial^2 v_0}{\partial r^2}-\frac{1}{r}\frac{\partial v_0}{\partial r}+\sum_{m=1}^{\infty}\Bigg[&\left(\frac{\partial\alpha_m}{\partial t}-\frac{\partial^2\alpha_m}{\partial r^2}-\frac{1}{r}\frac{\partial\alpha_m}{\partial r}+\frac{m^2}{r^2}\right)\cos m\theta\\&+\left(\frac{\partial\beta_m}{\partial t}-\frac{\partial^2\beta_m}{\partial r^2}-\frac{1}{r}\frac{\partial\beta_m}{\partial r}+\frac{m^2}{r^2}\right)\sin m\theta\Bigg]=0.\end{aligned} \tag{2.21}$$

The equation holds only when the coefficients of the series are equal to zero, which yields the following one-dimensional problems:

$$\frac{\partial v_0}{\partial t} - \frac{\partial^2 v_0}{\partial r^2} - \frac{1}{r}\frac{\partial v_0}{\partial r} = 0, \tag{2.22}$$

$$\frac{\partial \alpha_m}{\partial t} - \frac{\partial^2 \alpha_m}{\partial r^2} - \frac{1}{r}\frac{\partial \alpha_m}{\partial r} + \frac{m^2}{r^2} = 0, \quad m \geq 1, \tag{2.23}$$

$$\frac{\partial \beta_m}{\partial t} - \frac{\partial^2 \beta_m}{\partial r^2} - \frac{1}{r}\frac{\partial \beta_m}{\partial r} + \frac{m^2}{r^2} = 0, \quad m \geq 1. \tag{2.24}$$

After solving the above equations together with the corresponding initial and boundary conditions, we obtain a relationship between v, v_t and v_r on Γ [14],

$$\begin{aligned}\frac{\partial v(R,\theta,t)}{\partial r} &= -\frac{1}{2R\sqrt{\pi^3}}\int_0^t\int_0^{2\pi}\frac{\partial v(R,\phi,\tau)}{\partial \tau}d\phi\frac{H_0(t-\tau)}{\sqrt{t-\tau}}d\tau \\ &\quad -\frac{1}{R\sqrt{\pi^3}}\int_0^t\sum_{m=1}^{\infty}\int_0^{2\pi}\frac{\partial v(R,\phi,\tau)}{\partial \tau}\cos m(\phi-\theta)d\phi\frac{H_m(t-\tau)}{\sqrt{t-\tau}}d\tau \\ &\quad -\frac{1}{R\pi}\sum_{m=1}^{\infty} m\int_0^{2\pi} v(R,\phi,t)\cos m(\phi,\theta)d\phi,\end{aligned} \tag{2.25}$$

with

$$H_m(t) = \frac{4\sqrt{t}}{\sqrt{\pi^3}}\int_0^{\infty}\frac{e^{-\mu^2 t}}{J_m^2(\mu R)+Y_m^2(\mu R)}\frac{d\mu}{\mu}, \tag{2.26}$$

where $J_m(\cdot)$ and $Y_m(\cdot)$ are the Bessel functions of the first and second kinds of order m, respectively.

Taking the first M terms of the summation and transforming it back into the original variable, we obtain an approximate artificial boundary condition on Γ,

$$\begin{aligned}e^{u(R,\theta,t)}\frac{\partial u(R,\theta,t)}{\partial r} &\approx -\frac{1}{2R\sqrt{\pi^3}}\int_0^t\int_0^{2\pi}\frac{\partial e^{u(R,\phi,\tau)}}{\partial \tau}d\phi\frac{H_0(t-\tau)}{\sqrt{t-\tau}}d\tau \\ &\quad -\frac{1}{R\sqrt{\pi^3}}\int_0^t\sum_{m=1}^{M}\int_0^{2\pi}\frac{\partial e^{u(R,\phi,\tau)}}{\partial \tau}\cos m(\phi-\theta)d\phi\frac{H_m(t-\tau)}{\sqrt{t-\tau}}d\tau \\ &\quad -\frac{1}{R\pi}\sum_{m=1}^{M} m\int_0^{2\pi}(e^{u(R,\phi,t)}-1)\cos m(\phi,\theta)d\phi.\end{aligned} \tag{2.27}$$

For brevity, we write the approximating condition as

$$\frac{\partial u(R,\theta,t)}{\partial r} = \mathcal{K}_M(u,u_t). \tag{2.28}$$

It is obvious that when $M \to +\infty$, the boundary condition is exact. With this boundary condition, the original problem is reduced to an initial boundary value problem in the bounded domain Ω_i:

$$u_t = u_{rr} + u_r^2 + \frac{1}{r}u_r + \frac{1}{r^2}(u_{\theta\theta} + u_\theta^2) + f(r,\theta,t), \quad \text{in } \Omega_i \times (0,T] \tag{2.29}$$

$$u|_{\partial D} = g(r,\theta,t), \quad \text{in } \partial\Omega \times (0,T] \tag{2.30}$$

$$u(r,\theta,0) = u_0(r,\theta,0), \quad \text{in } \Omega_i, \tag{2.31}$$

$$\frac{\partial u(R,\theta,t)}{\partial r} = \mathcal{K}_M(u,u_t), \quad \text{on } \Gamma. \tag{2.32}$$

2.2 The three-dimensional KPZ equation

Under the spherical coordinates the KPZ equation in three dimensions is given by

$$\begin{aligned} u_t &= u_r^2 + u_{rr} + \frac{2}{r}u_r + \frac{1}{r^2}(u_\theta^2 + u_{\theta\theta} + \cot\theta u_\theta) \\ &\quad + \frac{1}{r^2\sin^2\theta}(u_\phi^2 + u_{\phi\phi}) + f(r,\theta,\phi,t). \end{aligned} \tag{2.33}$$

In the exterior domain $\Omega_e = \{(r,\theta,\phi) : r > R, \theta \in [0,\pi], \phi \in [0,2\pi]\}$, where the initial value $u(r,\theta,\phi,0)$ and the source term $f(r,\theta,\phi,t)$ vanish, the KPZ equation can also be transformed into a parabolic equation [23] by the Cole-Hopf transformation $v = e^u - 1$:

$$v_t = v_{rr} + \frac{2}{r}v_r + \frac{r^2}{\sin\theta}\frac{\partial}{\partial\theta}(\sin\theta v_\theta) + \frac{1}{r^2\sin^2\theta}v_{\phi\phi}. \tag{2.34}$$

The idea to obtain the artificial boundary condition is similar to that of the two-dimensional case. For the parabolic equation (2.34), the 3D problem can be solved using the Fourier series expansion. Let $P_m^l(\cdot)(m = 1,\cdots,l = 1,\cdots,m)$ be the associate Legendre functions in spherical coordinates. Then

$$\begin{aligned} P_m(\cos\gamma) &= P_m^0(\cos\xi)P_m^0(\cos\theta) \\ &\quad + 2\sum_{l=1}^{m}\frac{(m-l)!}{(m+l)!}P_m^l(\cos\xi)P_m^l(\cos\theta)\cos m(\psi-\phi), \end{aligned} \tag{2.35}$$

where $P_m(\cdot)$ is the Legendre polynomial of degree m, and γ, ξ and θ satisfy $\cos\gamma = \cos\xi\cos\theta + \sin\xi\sin\theta\cos(\psi-\phi)$. The relationship between v, v_t and v_r on $\Gamma = \{(r,\theta,\phi)|r =$

$R\}$ was found by Han and Yin [17],

$$\begin{aligned}
&\frac{\partial v(R,\theta,\phi,t)}{\partial r}\\
=\ & -\frac{1}{4\pi R}\int_S v(R,\xi,\psi,t)dS_{\xi,\psi} - \frac{1}{4\pi^{3/2}}\int_0^t\int_S \frac{\partial v(R,\xi,\psi,\tau)}{\partial \tau}dS_{\xi,\psi}\frac{1}{\sqrt{t-\tau}}d\tau\\
& -\sum_{m=1}^{\infty}\left[\frac{(m+1)(2m+1)}{4\pi R}\int_S v(R,\xi,\psi,t)P_m(\cos\gamma)dS_{\xi,\psi}\right.\\
& \left.+\frac{2m+1}{4\sqrt{\pi^3}}\int_0^t\int_S \frac{\partial v(R,\xi,\psi,\tau)}{\partial \tau}P_m(\cos\gamma)dS_{\xi,\psi}\frac{H_{m+\frac{1}{2}}(t-\tau)}{\sqrt{t-\tau}}d\tau\right] \qquad (2.36)
\end{aligned}$$

with

$$H_{m+\frac{1}{2}}(t)=\frac{4\sqrt{t}}{\sqrt{\pi^3}R}\int_0^\infty \frac{e^{-\mu^2 t}}{J^2_{m+\frac{1}{2}}(\mu R)+Y^2_{m+\frac{1}{2}}(\mu R)}\frac{d\mu}{\mu}.$$

Taking the first M terms of the summation and transforming back into the original variables, we obtain the approximate artificial boundary condition on Γ for the KPZ equation in 3D,

$$\begin{aligned}
&e^{u(R,\theta,\phi,t)}\frac{\partial u(R,\theta,\phi,t)}{\partial r}\\
=\ & -\frac{1}{4\pi R}\int_S (e^{u(R,\xi,\psi,t)}-1)dS_{\xi,\psi} - \frac{1}{4\pi^{3/2}}\int_0^t\int_S \frac{\partial e^{u(R,\xi,\psi,\tau)}}{\partial \tau}dS_{\xi,\psi}\frac{1}{\sqrt{t-\tau}}d\tau\\
& -\sum_{m=1}^{M}\left[\frac{(m+1)(2m+1)}{4\pi R}\int_S (e^{u(R,\xi,\psi,t)}-1)P_m(\cos\gamma)dS_{\xi,\psi}\right.\\
& \left.+\frac{2m+1}{4\sqrt{\pi^3}}\int_0^t\int_S \frac{\partial e^{u(R,\xi,\psi,\tau)}}{\partial \tau}P_m(\cos\gamma)dS_{\xi,\psi}\frac{H_{m+\frac{1}{2}}(t-\tau)}{\sqrt{t-\tau}}d\tau\right]. \qquad (2.37)
\end{aligned}$$

Again for brevity, we write the approximating condition as

$$\frac{\partial u(R,\theta,\phi,t)}{\partial r}=\mathcal{K}_M(u,u_t).$$

3 Numerical approximation

We consider the numerical approximation of the reduced problem in the two-dimensional case. In the computational region $[a,R]\times[0,2\pi]$, let $\Delta r=(R-a)/I$ and $\Delta\theta=2\pi/J$ be the spatial mesh size in r and θ, respectively, and let $\Delta t=\frac{T}{N}$ be the time step, where I,J and N are positive integers. Let the grid points and temporal mesh points be

$$r_i=a+i\Delta r,\quad \theta_j=j\Delta\theta,\quad t_n=n\Delta t,$$

and denote the approximation of $u(r_i,\theta_j,t_n)$ by u_{ij}^n.

For the approximation of the KPZ equation, we use the second-order implicit Crank-Nicolson scheme,

$$\begin{aligned}
&\frac{u_{ij}^{n+1}-u_{ij}^n}{\Delta t}\\
=\;&\frac{u_{i+1,j}^{n+\frac12}-2u_{i,j}^{n+\frac12}+u_{i-1,j}^{n+\frac12}}{\Delta r^2}+\frac{(u_{i+1,j}^{n+1}-u_{i-1,j}^{n+1})^2+(u_{i+1,j}^{n}-u_{i-1,j}^{n})^2}{8\Delta r^2}\\
&+\frac{u_{i+1,j}^{n+\frac12}-u_{i-1,j}^{n+\frac12}}{r_i\Delta r}+\frac{u_{i,j+1}^{n+\frac12}-2u_{i,j}^{n+\frac12}+u_{i,j-1}^{n+\frac12}}{r_i^2\Delta\theta^2}\\
&+\frac{(u_{i,j+1}^{n+1}-u_{i,j-1}^{n+1})^2+(u_{i,j+1}^{n}-u_{i,j-1}^{n})^2}{8r_i^2\Delta\theta^2}+f(r_i,\theta_j,t_{n+1/2}),
\end{aligned}\tag{3.1}$$

with initial and boundary conditions

$$u_{ij}^0=u_0(r_i,\theta_j,0),\quad u_{0,j}^n=g(a,\theta_j,t_n),\quad u_{i,0}^n=u_{i,J}^n,\tag{3.2}$$

where

$$u_{ij}^{n+\frac12}=\frac12(u_{ij}^{n+1}+u_{ij}^n).$$

On the artificial boundary Γ, we follow the method proposed in Han and Huang [14] to discretize the integrals,

$$\begin{aligned}
&\int_{\mathcal{D}_n}\frac{\partial e^{u(R,\phi,\tau)}}{\partial\tau}d\phi\frac{H_0(t_n-\tau)}{t_n-\tau}d\tau\\
=\;&\sum_{l=0}^{n}\sum_{s=0}^{J-1}\frac{\Delta\theta}{\Delta t}(e^{u_{I,s}^{l+1}}-e^{u_{I,s}^{l}})\int_{t_l}^{t_{l+1}}\frac{H_0(t_{n+1}-\tau)}{\sqrt{t_{n+1}-\tau}}d\tau,
\end{aligned}\tag{3.3}$$

$$\begin{aligned}
&\int_{\mathcal{D}_n}\frac{\partial e^{u(R,\phi,\tau)}}{\partial\tau}\cos m(\phi-\theta_j)d\phi\frac{H_m(t_n-\tau)}{t_n-\tau}d\tau\\
=\;&\frac{1}{m^2\Delta\theta\Delta t}\sum_{l=0}^{n}\sum_{s=0}^{J-1}(e^{u_{I,s}^{l+1}}-e^{u_{I,s}^{l}})\Big[2\cos m(\theta_s-\theta_j)-\cos m(\theta_{s+1}-\theta_j)\\
&\qquad-\cos m(\theta_{s-1}-\theta_j)\Big]\int_{t_l}^{t_{l+1}}\frac{H_m(t_{n+1}-\tau)}{\sqrt{t_{n+1}-\tau}}d\tau,
\end{aligned}\tag{3.4}$$

where $\mathcal{D}_n=[0,2\pi]\times[0,t_{n+1}]$; and

$$\begin{aligned}
\int_0^{2\pi}(e^{u(R,\phi,t_{n+1})}-1)\cos m(\phi-\theta_j)d\phi&=\frac{1}{m^2\Delta\theta}\sum_{s=0}^{J-1}(e^{u_{I,s}^{n+1}}-1)\\
&\times\Big[2\cos m(\theta_s-\theta_j)-\cos m(\theta_{s+1}-\theta_j)-\cos m(\theta_{s-1}-\theta_j)\Big].
\end{aligned}\tag{3.5}$$

Since the above system is implicit, we must use an iterative method to solve it numerically. Here a simple iteration method is used in our numerical experiments. At each iteration step, we approximate the nonlinear term of (3.1) by

$$(u_{i+1,j}^{n+1}-u_{i-1,j}^{n+1})^2=(u_{i+1,j}^{n+1}-u_{i-1,j}^{n+1})^{(k)}(u_{i+1,j}^{n+1}-u_{i-1,j}^{n+1})^{(k+1)},$$
$$(u_{i,j+1}^{n+1}-u_{i,j-1}^{n+1})^2=(u_{i,j+1}^{n+1}-u_{i,j-1}^{n+1})^{(k)}(u_{i,j+1}^{n+1}-u_{i,j-1}^{n+1})^{(k+1)},$$

where the superscript k denotes the k-th iteration for solving the nonlinear difference equations at each time step. The initial iteration is chosen as $(u_{ij}^{n+1})^{(0)}=u_{ij}^n$.

Furthermore, in order to improve the convergence speed, we approximate the kernels of (3.3) and (3.4) in the region $[t_n,t_{n+1}]$ as follows:

$$e^{u_{I,s}^{n+1}}-e^{u_{I,s}^n}=\left[(u_{I,s}^{n+1})^{(k+1)}-u_{I,s}^n\right]\frac{1}{2}\left(e^{(u_{I,s}^{n+1})^{(k)}}+e^{u_{I,s}^n}\right). \tag{3.6}$$

Moreover, $e^{u_{I,s}^{n+1}}$ in (3.5) is approximated by the k-th iteration value. Finally, a related problem is the computation of the integral

$$\int_{t_l}^{t_{l+1}}\frac{H_m(\tau)}{\sqrt{\tau}}d\tau=\frac{4}{\sqrt{\pi^3}}\int_0^\infty\frac{\int_{t_l}^{t_{l+1}}e^{-\mu^2\tau}d\tau}{J_m^2(\mu R)+Y_m^2(\mu R)}\frac{d\mu}{\mu}.$$

The integral kernel decays slowly which reduces the computational efficiency. Fortunately, this integral is independent of the variable u. Therefore, we can make some tables before starting the numerical computations.

4 Numerical examples

To show the effectiveness of the new approach using artificial boundaries, we present some two-dimensional numerical examples in this section.

Example 4.1. Consider the following initial boundary value problem in the domain in the exterior of a circle:

$$u_t=u_{rr}+u_r^2+\frac{1}{r}u_r+\frac{1}{r^2}(u_{\theta\theta}+u_\theta^2),\quad \text{for } r>a \tag{4.1}$$
$$u(a,\theta,t)=g(\theta,t), \tag{4.2}$$
$$u(r,\theta,0)=0, \tag{4.3}$$

with $a=2$ and

$$g(\theta,t)=\log\left[\frac{1}{t}\exp\left(-\frac{(a\cos\theta-x_0)^2+(a\sin\theta-y_0)^2}{4t}\right)+1\right],$$

where $(x_0,y_0)=(0.5,0.5)$. The exact solution of the problem is

$$u(r,\theta,t)=\log\left[\frac{1}{t}\exp\left(-\frac{(r\cos\theta-x_0)^2+(r\sin\theta-y_0)^2}{4t}\right)+1\right].$$

We introduce the artificial boundary $\Gamma=\{(r,\theta):r=R,0\le\theta<2\pi\}$ with $R=3$.

Table 1: Example 4.1: L_1 errors and orders of accuracy.

M	$I \times J$	Error	Order	M	$I \times J$	Error	Order
0	4×24	1.82e-2	–	3	4×24	2.15e-3	–
	8×48	1.72e-2	0.08		8×48	1.07e-3	1.00
	12×72	1.68e-2	0.06		12×72	5.86e-4	1.48
	16×96	1.67e-2	0.06		16×96	4.40e-4	1.00
1	4×24	6.76e-3	–	4	4×24	2.15e-3	–
	8×48	6.31e-3	0.10		8×48	9.24e-4	1.22
	12×72	5.94e-3	0.15		12×72	3.85e-4	2.16
	16×96	5.86e-3	0.05		16×96	2.11e-4	2.09
2	4×24	2.89e-3	–	5	4×24	2.15e-3	–
	8×48	2.16e-3	0.42		8×48	9.21e-4	1.22
	12×72	1.73e-3	0.55		12×72	3.76e-4	2.21
	16×96	1.61e-3	0.25		16×96	1.97e-4	2.25

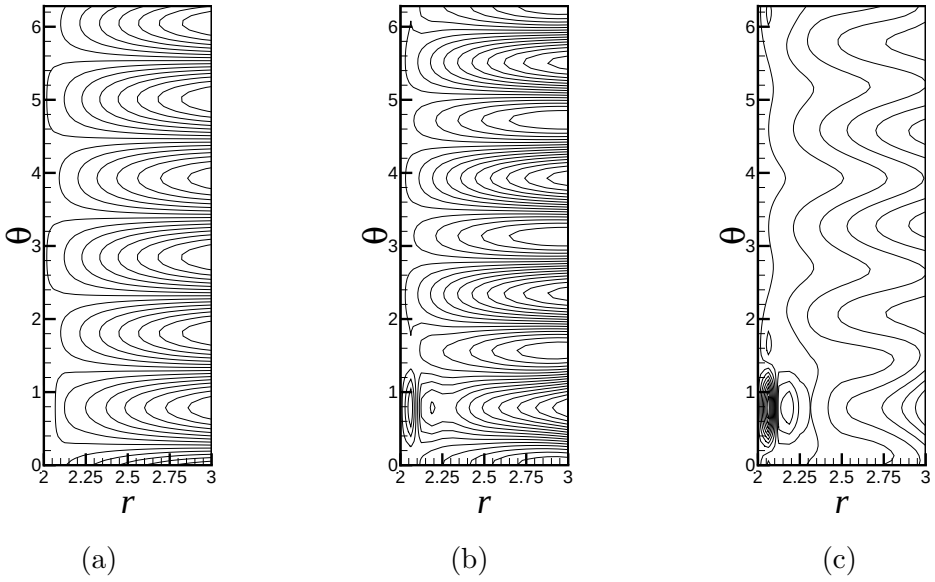

(a) (b) (c)

Figure 1: Errors at T for Example 4.1, with $I = 16$: (a) $N = 2$, with 15 contours from -3.85×10^{-3} to 4.04×10^{-3}; (b) $N = 3$, with 15 contours from -2.82×10^{-4} to 5.74×10^{-4}; (c) $N = 4$, with 15 contours from -2.21×10^{-4} to 1.89×10^{-4}.

Taking $\Delta r = \frac{1}{I}$, $\Delta\theta = \frac{2\pi}{6I}$, $\Delta t = \Delta r$, and $T = 1$, we show the numerical errors and orders of accuracy in Table 1 with different truncation order M. Here the L_1-error E_1 is

defined by

$$E_1 = \frac{1}{(I+1)(J+1)(N+1)} \sum_{n=0}^{N} \sum_{i=0}^{I} \sum_{j=0}^{J} |u(r_i, \theta_j, t^n) - u_{ij}^n|.$$

We can see that the numerical errors decrease fast with increasing values of the truncation order M. When $M \geq 4$, the order of convergence is close to 2. Fig. 1 shows the spatial distribution of errors at $t = T$ for $M = 2, 3$ and 4, respectively.

Example 4.2. To see the relation between the numerical errors and the truncation order M more clearly, we consider the same problem as in Example 4.1 with different interior boundary condition,

$$g(\theta, t) = (1 - e^{-\frac{3}{2}t}) \cos \omega\theta.$$

Here ω represents the frequency of the oscillation. The artificial boundary is also introduced on $\Gamma = \{(r, \theta) : r = R, 0 \leq \theta < 2\pi\}$ with $R = 3$. In all numerical experiments, we take $\Delta r = \frac{1}{I}$, $\Delta\theta = \frac{2\pi\omega}{6I}$, $\Delta t = \Delta r$, and $T = 1$. So for different frequencies and the same I, the grid point distribution in one wavelength is the same.

We obtain relative errors by comparing the solutions obtained with $R = 3$ and $R = 8$ with the same mesh size. The error is computed on the artificial boundary Γ (i.e. $R = 3$) at time $t = T$. We show the results with $I = 8$ and the frequency modes $\omega = 1, 2$ and 3 in Figs. 2-4, respectively. It is observed that the solution converges very fast as M increases. It is also observed that larger values of M are needed when the frequency ω becomes larger.

Example 4.3. In this example, we consider the KPZ equation with a source term in the domain outside of a circle,

$$u_t = u_{rr} + u_r^2 + \frac{1}{r} u_r + \frac{1}{r^2}(u_{\theta\theta} + u_\theta^2) + f(r, \theta, t), \quad \text{for } r > a \tag{4.4}$$

$$u(a, \theta, t) = (1 - e^{-t}) \sin \frac{\pi t}{4}, \tag{4.5}$$

$$u(r, \theta, 0) = 0, \tag{4.6}$$

with $a = 2$ and the source term

$$f(r, \theta, t) = e^{-5(r-4)^2} \sin(\frac{\pi t}{4}) \sin \theta,$$

which decays rapidly in r. We introduce the artificial boundary on $\Gamma = \{(r, \theta) : r = R, 0 \leq \theta < 2\pi\}$ with $R = 6$. Outside of Γ, the source term is almost zero; thus we can use the artificial boundary method to solve this problem in a bounded domain $\{(r, \theta) | r < R\}$.

In out computations, we take $\Delta r = \frac{4}{I}$, $\Delta\theta = \frac{2\pi}{J}$, $\Delta t = \Delta r$, and $T = 8$. Figs. 5 and 6 show the solution for different gird sizes at time $t = 4$ and 8 using the approximating boundary condition with $M = 4$. We can see that the artificial boundary method can solve this problem very well. In particular, almost no reflecting waves are produced near the artificial boundary.

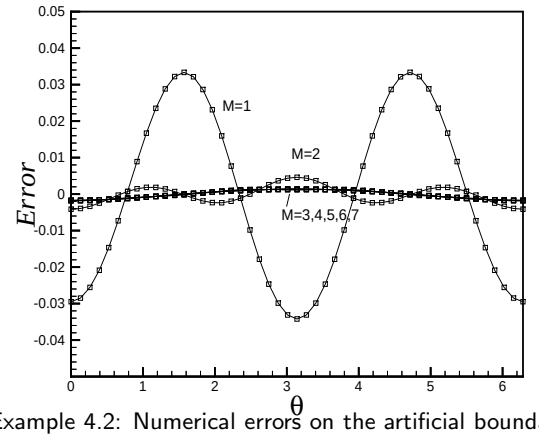

Figure 2: Example 4.2: Numerical errors on the artificial boundary, with $\omega = 1$.

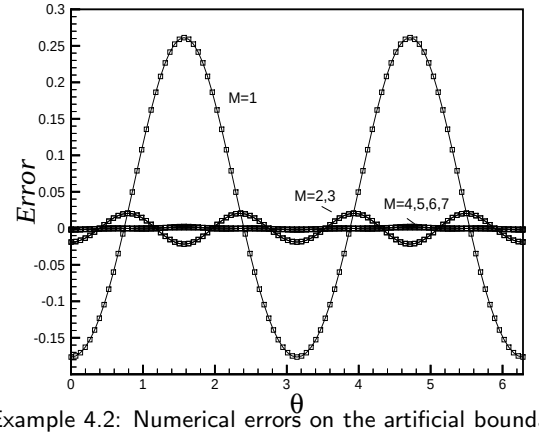

Figure 3: Example 4.2: Numerical errors on the artificial boundary, with $\omega = 2$.

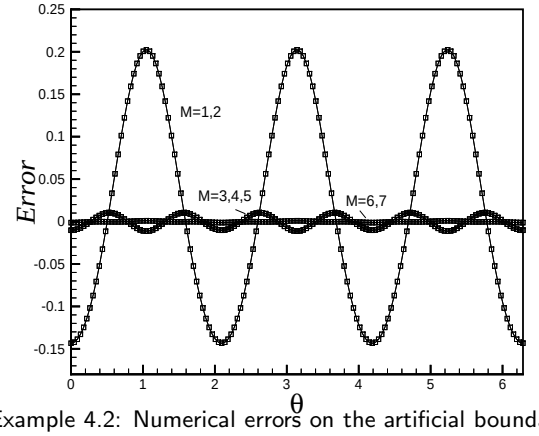

Figure 4: Example 4.2: Numerical errors on the artificial boundary, with $\omega = 3$.

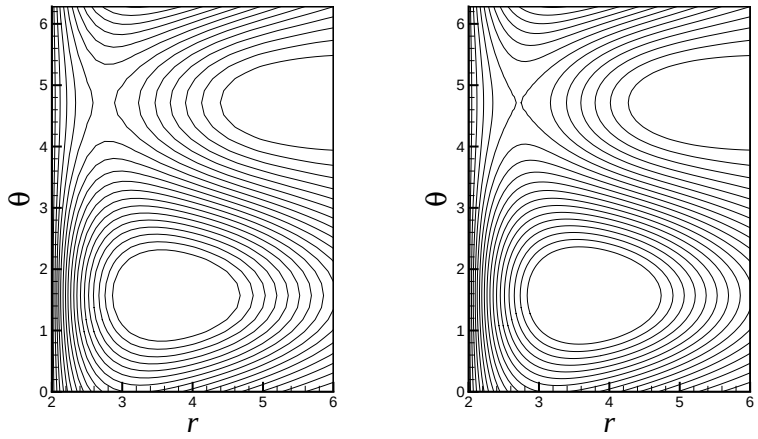

32×32 64×64

Figure 5: Example 4.3: u values at $t = 4$, with 20 contour lines ranging from -0.04 to 0.54.

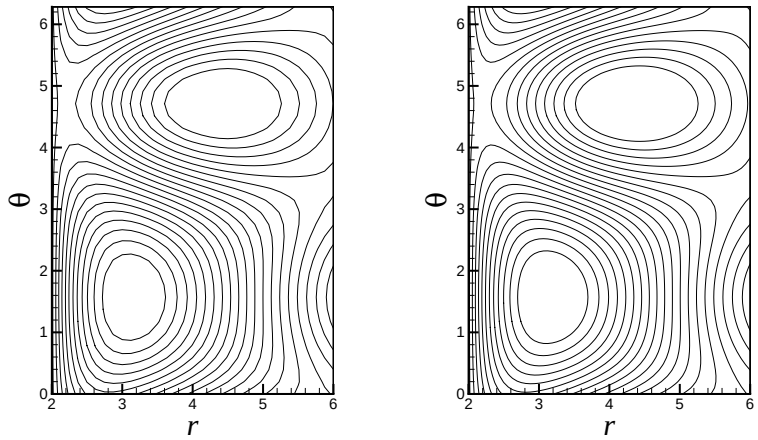

32×32 64×64

Figure 6: Example 4.3: u values at $t = 8$, with 20 contours lines ranging from -0.28 to 0.19.

5 Conclusion

In this paper, the artificial boundary method is applied to the nonlinear Kardar-Parisi-Zhang equation in one-, two- and three-dimensional unbounded domains. With the Cole-Hopf transformation, we are able to obtain the boundary conditions on the artificial boundaries. These boundary conditions are in nonlinear forms. The original problems are reduced to equivalent problems in bounded domains. This procedure is similar to the

artificial boundary method for linear problems. Numerical examples demonstrate that this reduction is very effective, and high accuracy can be obtained by using relatively small computational domains.

Acknowledgments

Research is supported in part by National Natural Science Foundation of China, Hong Kong Research Grants Council and FRG of Hong Kong Baptist University.

References

[1] M. Beccaria and G. Curci, Numerical simulation of the Kardar-Parisi-Zhang equation, Phys. Rev. E, 50 (1994), pp. 4560–4563.
[2] S. Bryson and D. Levy, Central schemes for multidimensional Hamilton-Jacobi equations, SIAM J. Sci. Comput., 25 (2003), 767–791.
[3] B. Engquist and A. Majda, Absorbing boundary conditions for the numerical simulation of waves, Math. Comput., 31 (1977), 629–651.
[4] K. Feng, Differential vs. integral equations and finite vs. infinite elements, Math. Numer. Sinica, 2 (1980), 100–105.
[5] G. N. Gatica and S. Meddahi, A fully discrete Galerkin scheme for a two-fold saddle point formulation of an exterior nonlinear problem, Numer. Funct. Anal. Optimiz., 22 (2001), 885–912.
[6] L. Giada, A. Giacometti and M. Rossi, Pseudospectral method for the Kardar-Parisi-Zhang equation, Phys. Rev. E, 65 (2002), 036134.
[7] L. Greengard and P. Lin, Spectral approximation of the free-space heat kernel, Appl. Comput. Harmon. Anal., 9 (2000), 83–97.
[8] M. J. Grote and J. B. Keller, On nonreflecting boundary conditions, J. Comput. Phys., 122 (1995), 231–243.
[9] T. Hagstrom, S. I. Hariharan and D. Thompson, High-order radiation boundary conditions for the convective wave equation in exterior domains, SIAM J. Sci. Comput., 25 (2003), 1088–1101.
[10] T. Hagstrom and H. B. Keller, Asymptotic boundary conditions and numerical methods for nonlinear elliptic problems on unbounded domains, Math. Comput., 48 (1987), 449–470.
[11] H. Han and X. N. Wu, Approximation of infinite boundary condition and its applications to finite element methods, J. Comput. Math., 3 (1985), 179–192.
[12] H. Han and X. N. Wu, The approximation of the exact boundary conditions at an artificial boundary for linear elastic equations and its application, Math. Comput., 59 (1992), 21–37.
[13] H. D. Han and Z. Y. Huang, A class of artificial boundary conditions for heat equation in unbounded domains, Comput. Math. Appl., 43 (2002), 889–900.
[14] H. D. Han and Z. Y. Huang, Exact and approximating boundary conditions for the parabolic problems on unbounded domains, Comput. Math. Appl., 44 (2002), 655–666.
[15] H. D. Han, J. F. Lu and W. Z. Bao, A discrete artificial boundary condition for steady incompressible viscous flows in a no-slip channel using a fast iterative method, J. Comput. Phys., 114 (1994), 201–208.
[16] H. D. Han, X. N. Wu and Z. L. Xu, Artificial boundary method for Burgers' equation using nonlinear boundary conditions, preprint.

[17] H. D. Han and D. S. Yin, Numerical solutions of parabolic problems on unbounded 3-D spatial domain, J. Comput. Math., 23 (2005), 449–462.
[18] M. Kardar, G. Parisi and Y. C. Zhang, Dynamic scaling of growing interfaces, Phys. Rev. Lett., 56 (1986), 889–892.
[19] J. B. Keller and D. Givoli, Exact nonreflecting boundary conditions, J. Comput. Phys., 82 (1989), 172–192.
[20] C. H. Lam and F. G. Shin, Improved discretization of the Kardar-Parisi-Zhang equation, Phys. Rev. E, 58 (1998), 5592.
[21] J. Strain, Fast adaptive methods for the free-space heat equation, SIAM J. Sci. Comput., 15 (1994), 185–206.
[22] T. Vicsek, Fractal Growth Phenomena, 2nd ed., World Scientific, 1992.
[23] G. B. Whitham, Linear and Nonlinear Waves, John Wiley & Sons, Inc., 1974.
[24] X. N. Wu and Z. Z. Sun, Convergence of difference scheme for heat equation in unbounded domains using artificial boundary conditions, Appl. Numer. Math., 50 (2004), 261–277.
[25] D. H. Yu, Approximation of boundary conditions at infinity for a harmonic equation, J. Comput. Math., 3 (1985), 219–227.
[26] Y. T. Zhang and C.-W. Shu, High-order WENO schemes for Hamilton-Jacobi equations on triangular meshes, SIAM J. Sci. Comput., 24 (2003), 1005–1030.